Ordered Nanosheet-Based $YBO_3:Eu^{3+}$ Assemblies: Synthesis and Tunable Luminescent Properties

Xiao-Cheng Jiang, Ling-Dong Sun, and Chun-Hua Yan*

State Key Laboratory of Rare Earth Materials Chemistry and Applications, PKU-HKU Joint Laboratory on Rare Earth Materials and Bioinorganic Chemistry, College of Chemistry & Molecular Engineering, Peking University, Beijing 100871, China

Received: October 31, 2003; In Final Form: January 23, 2004

Uniform donut-like assemblies of $YBO_3:Eu^{3+}$ were obtained via a simple hydrothermal method, in the absence of any surfactant or template. These microparticles were actually composed of orderly aggregated nanosheets and exhibited improved chromaticity compared with the bulk. After controlled postcalcination, the microstructure of the assembly experienced great changes and the correspondent luminescent properties also showed interesting evolution, but the assembled particle size stayed the same. This was very important for their potential application in devices. Because the previous size-dependent properties were localized to the same scale, the performance of these devices could be easily tuned by simple calcination, without destroying the particle arrangement and physical appearance.

Introduction

With the progress of nanoscience, people are now equipped with various fabrication methods toward functional materials with novel properties on the nanoscale level. These so-called "size-dependent properties" are of great interest and significance, but to realize their potential application in appropriate devices, controlled construction of these nanosized units into orderly structures is becoming a key problem and new challenge. In such constructions, copolymers and surfactants always play important roles[1−3] due to their directing functions during the aggregation process as well as their stabilizing effects in equilibrium systems. Actually, the process is complicated, and the resulting structures are always not stable enough for practical uses. From a technical viewpoint, a simple, clean, and controllable approach toward durable structures, is desired. However, up to now, the knowledge about surfactant-free assembly of nanomaterials is still of great lack. [4]

In spite of this fact, most nanomaterials often show a natural tendency toward aggregation. This is always assumed as the main hindrance to their practical application. Rare earth orthoborates ($REBO_3$), which are apt to form highly agglomerated particles,[5] are representative. Represented by YBO_3:Eu, these materials are finding applications in a wide range of optical applications ranging from phosphors to high-damage threshold ultraviolet optical components.[6,7] From a standpoint of materials chemistry and physics, they represent interesting systems to test and develop fundamental ideas about synthesis and properties of doped-insulators. Despite their importance, the research about the synthesis and morphology control is far from sufficient compared with other materials,[6,8−13] such as metals and semiconductors, resulting from the fact that they are high-temperature phased species that are very difficult to prepare and get in control. However, from the aspect of nanotectonics,[14] $REBO_3$ nanocrystals may be ideal building blocks, because they will result in assemblies with especially high stability, as can be forecasted from their unusual aggregation tendency.

* Corresponding author. Tel. & Fax: +86-10-62754179. E-mail: chyan@chem.pku.edu.cn.

The foremost problem of building such assemblies lies in the organization of these unstable building blocks. Our present work exhibited that through a simple hydrothermal process under appropriate conditions, self-assembled $YBO_3:Eu^{3+}$ microparticles with high order and stability could be obtained. These microparticles, which were composed of nanosized units, were expected to maintain the desirable properties of $YBO_3:Eu^{3+}$ nanocrystals while being quite stable on the micrometer-scale; thus its luminescent properties can be further adjusted without changing its assembled-particle size, through the altering of its crystallization degree by controlling the calcination process.

Experimental Section

Appropriate amounts of Y_2O_3, Eu_2O_3 (Y:Eu = 9:1, in molar ratio) and H_3BO_3 (100% excess) were dissolved in dilute HNO_3, controlling the total concentration of metal cation to be 0.05 mol/L. Under vigorous stirring, $NH_3 \cdot H_2O$ solution (1:1 in v/v) was added dropwise until the pH value of the stock solution was adjusted to 8. A given volume (85 mL) of the milky gel was then transferred into a Teflon bottle (100 mL) held in a stainless steel autoclave and was placed in a temperature-controlled electric oven, heated at 180 °C for 6 h. As the autoclave cooled to room-temperature naturally, the precipitates were separated by centrifugation, washed with deionized water and ethanol several times, and then dried in a vacuum oven at about 80 °C for 12 h. The resulting phosphors were then calcined at 700−1100 °C for 5 h. The bulk $YBO_3:Eu^{3+}$ was obtained by a direct solid-state reaction (SR) from the mixture of Y_2O_3, Eu_2O_3, and H_3BO_3 at 1100 °C for 10 h in air. X-ray diffraction (XRD) studies were carried out on a Rigaku D/max-2000 X-ray powder diffractometer using Cu $K\alpha$ ($\lambda = 1.5418$ Å) radiation. The size and morphology of the products were characterized by scanning electron microscopy (SEM, AMARY 1910FE) at 15 kV. Fluorescence spectra were recorded on a Hitachi F-4500 spectrophotometer equipped with a 150 W Xe-arc lamp at room temperature. The emission spectra were measured at a fixed band-pass of 0.2 nm with the same instrument parameters for comparison of different samples.

10.1021/jp037301q CCC: $27.50
Published on Web 02/25/2004

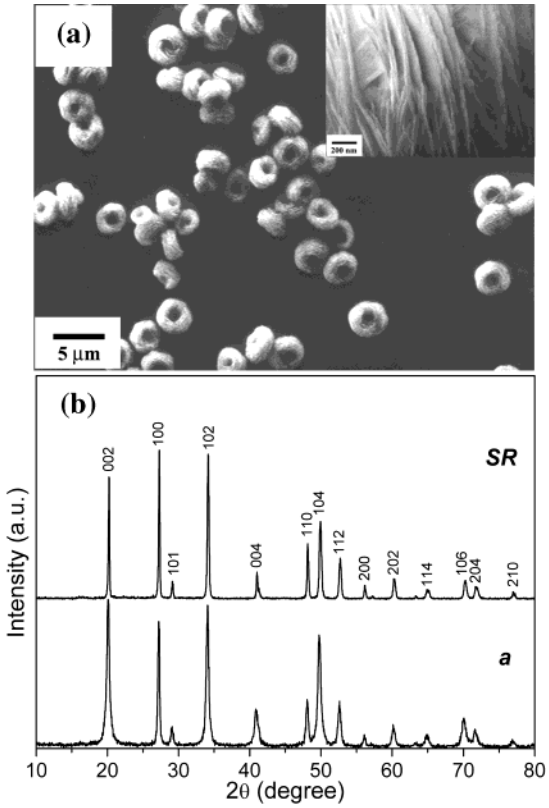

Figure 1. (a) SEM images of sample *a*, which was prepared by a hydrothermal method at 180 °C. The inset is a magnification of the edge of a single "donut". (b) XRD patterns for sample *a* and SR (the sample prepared by a direct solid-state reaction).

Results and Discussion

The typical SEM image of as-prepared sample (denoted as ***a***) is shown in Figure 1a, from which we can clearly observe the uniform donut-like microparticles whose diameters are about 3 μm. These particles were so stable that even under harsh ultrasonic conditions for a long time, there was no evidence for any collapse or change. By pursuing the shape evolution by stepwise prolonging the reaction time, we found that the formation of these donut-like microparticles followed a homocentric growth mechanism. A magnified image of the side of these microparticles is presented in the inset, which exhibited that they were actually based on the oriented assembly of numerous nanosheets whose thickness was around 10 nm. This observation coincided with the XRD pattern of *a*, as shown in Figure 1b. Although all the peaks could be well indexed to the hexagonal phase of YBO_3 with vaterite-type (JCPDS 16-277), they had quite different broadening behavior compared with those of the bulk synthesized through a solid-state reaction (SR). The peak (002), for example, was far broader than the peak (100), which is the characteristic of two-dimensional nanomaterials. This also indicates that the assembly was composed of single sheets but not nanoparticles.

The emission spectra of sample *a* and SR under 240 nm UV excitation are shown in Figure 2. The sharp lines ranging from 580 to 720 nm are associated with the transitions from the excited $^5D_0$ level to ^7F_J ($J = 1-4$) levels of Eu^{3+} activators.[15,16] As can be obviously seen, the ratio of the red emission at 610 nm to the orange emission at 591 nm (R/O value) of *a* is much higher than that of SR, which meant that an improved chromaticity can be obtained in these donut-like assemblies. This improvement was especially important for a red phosphor like $YBO_3:Eu^{3+}$, whose application was always restricted by its relatively poor chromaticity. We attribute this improvement to the distinct microstructure of the assembly, which maintains the characteristics of the building blocks—nanosheets. These nanosheets possess especially large surface area and high surface energy, which would not only form the main impetus for assembly but also result in a high degree of disorder and correspondent lower symmetry of crystal field around Eu^{3+} ions. As predicted by Judd−Ofelt theory,[17] a lower symmetry of the crystal field will result in a higher R/O value. On the basis of this comprehension, the improved chromaticity of the assembly is indeed correlated with the microstructure and crystallinity, but not the assembled particle size. By changing its microstructure and degree of crystallization via controlled postcalcination, we may effectively adjust its luminescent properties while maintaining the assembled particle size.

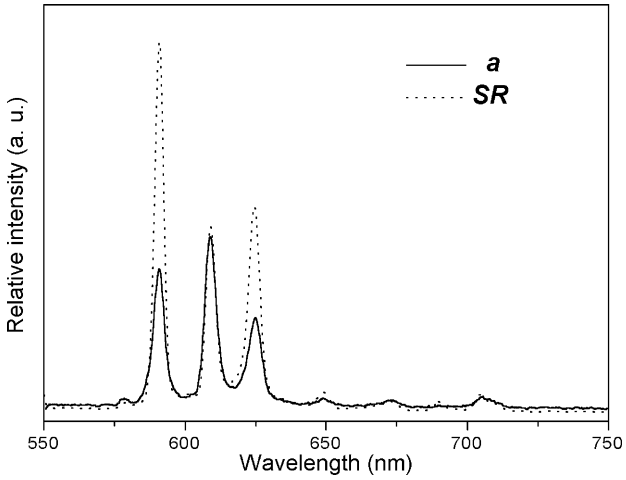

Figure 2. Emission spectra of samples *a* and SR under 240 nm UV excitation.

Parts b−d of Figure 3 exhibit the SEM images of sample *a* after calcination at 700, 900, and 1100 °C for 5 h, respectively. For comparison, a magnified image of *a* before calcination is also included and shown in Figure 3a. We can see that through calcination, the microstructure experiences great changes although the assembled particle size and external shape stay the same. When calcined at 700 °C, as can be seen in Figure 3b, the nanosheets begin to fuse with each other and form thicker sheets with better crystallinity. When the calcination temperature is increased to 900 °C, however, the characteristic morphology of nanosheets no longer exists. Under this high temperature, the relatively high surface energy of nanosheets may cause them to be partly melted and the surface tension results in the sphere-like morphology. These small particles are highly cross-linked and form honeycomblike structures. When the temperature is further increased to 1100 °C, the morphology shows no major changes. But the crystallinity, without doubt, can be greatly improved.

Normalized emission spectra of sample *a* with different calcination temperatures under 240 nm excitation are shown in Figure 4, and the change of luminescent intensity versus calcination temperature is summarized in the inset. With the increase of the calcination temperature, the emission spectrum of sample *a* experiences interesting changes. Both the red emission at 610 nm and the orange emission at 591 nm are strengthened as a result of the better crystallization. However, the increase of the orange emission is much faster than the red one, and accordingly, the R/O value decreases with temperature. This change is in accordance with the transformation of the microstructure of the assembly and aforementioned explanations. With increasing calcination temperature, poor-crystallized

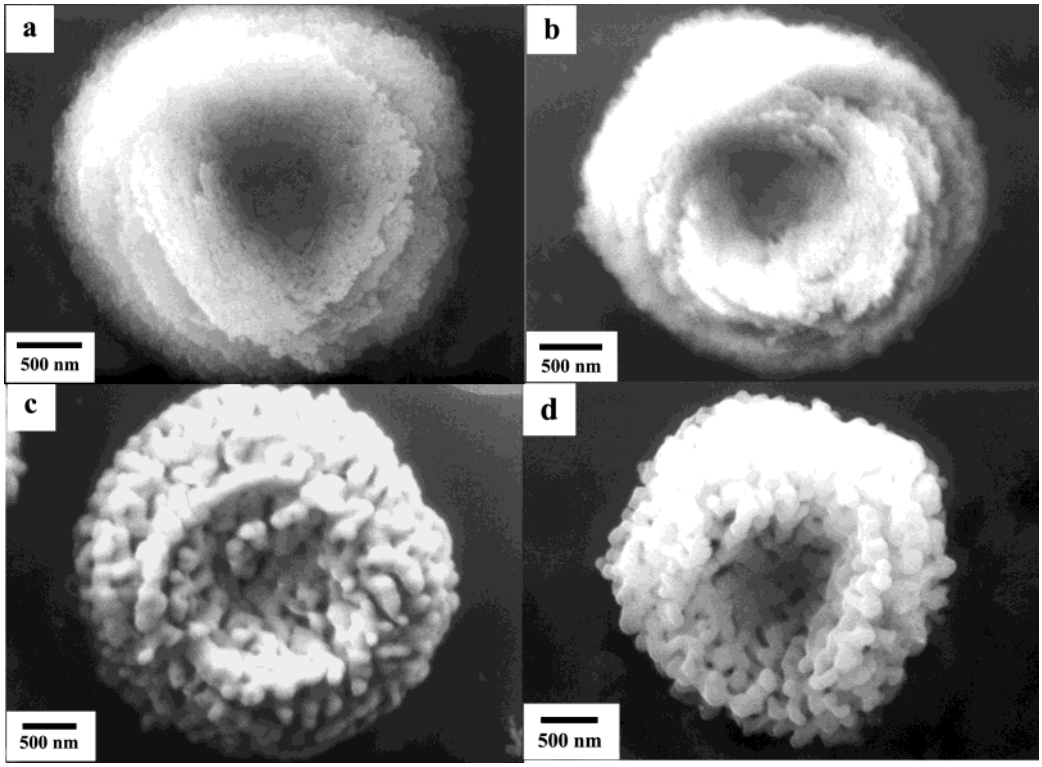

Figure 3. SEM images of sample *a* before calcination (a) and after calcination at 700 °C (b), 900 °C (c), and 1100 °C (d), respectively.

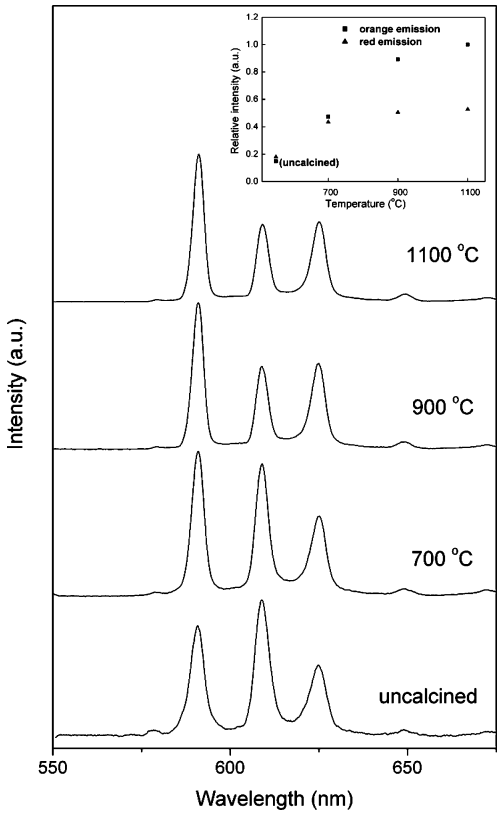

Figure 4. Normalized emission spectra of sample *a* with different calcination temperatures under 240 nm excitation. The inset describes the evolution of the relative intensity of the orange emission at 591 nm and the red emission at 610 nm versus calcination temperature.

nanosheets evolve into well-crystallized cross-linked particles. The improved crystallinity, as discussed above, will lower the R/O value. Here we afford the possibility of covering the properties from the characteristics of nanocrystals to bulk without changing the assembled particle size. This was very important for their potential application in devices. From a technical point of view, 700 °C may be the proper calcination temperature, because when the temperature was further increased, the enhancement of the luminescent intensity of red emission was little compared with the deterioration of chromaticity.

In summary, we prepared donut-like $YBO_3:Eu^{3+}$ assemblies with good unifromity and stability via a simple hydrothermal method. These microparticles possess improved performance compared with the bulk, and by changing the calcination temperature, their microstructure and correspondent luminescent properties can be efficiently tuned, without destroying the external shape or changing the assembled particle size. Our results showed that utilizing the strong interparticle interactions in highly agglomerated materials to build ordered assemblies was an economical choice, and the resulting exceptional stability brings the possibility of covering the properties from the characteristics of nanocrystals to bulk, on the same scale.

Acknowledgment. This work is supported by the NSFC (20221101 and 10374006), MOST (G19980613), MOE (the Foundation for University Key Teacher), the Founder Foundation of PKU, and Hui-Chun Chin and Tsung-Dao Lee Chinese Undergraduate Research Endowment (CURE).

References and Notes

(1) Boal A. K.; Ilhan F.; DeRouchey J. E.; Thurn-Albrecht T.; Russell T. P.; Rotello V. M. *Nature* **2000**, *404*, 746.

(2) Leontidis E.; Orphanou M.; Kyprianidou-Leodidou T.; Krumeich F.; Caseri W. *Nano Lett.* **2003**, *3*, 569.

(3) Naik S. P.; Chiang A. S. T.; Thompson R. W.; Huang F. C. *Chem. Mater.* **2003**, *15*, 787.

(4) Yuan J. K.; Laubernds K.; Zhang Q. H.; Suib S. L. *J. Am. Chem. Soc.* **2003**, *125*, 4966.

(5) Wei Z. G.; Sun L. D.; Liao C. S.; Jiang X. C.; Yan C. H. *J. Mater. Chem.* **2002**, *12*, 3665.

(6) Ren M.; Lin J. H.; Dong Y.; Yang L. Q.; Su M. Z.; You L. P. *Chem. Mater.* **1999**, *11*, 1576.

(7) Yang Z.; Ren M.; Lin J. H.; Su M. Z.; Tao Y.; Wang W. *Chem. J. Chin. U.* **2000**, *21*, 1339.
(8) Kim D. S.; Lee R. Y. *J. Mater. Sci.* **2000**, *35*, 4777.
(9) Boyer D.; Bertrand-Chadeyron G.; Mahiou R.; Caperaa C.; Cousseins J. C. *J. Mater. Chem.* **1999**, *9*, 211.
(10) Li Y. Y.; Peng M. L.; Feng S. H. *Chin. Chem. Lett.* **1996**, *7*, 387.
(11) Kim K. N.; Jung H. K.; Park H. D.; Kim D. *J. Mater. Res.* **2002**, *17*, 907.
(12) Wei Z. G.; Sun L. D.; Liao C. S.; Yan C. H. *Appl. Phys. Lett.* **2002**, *80*, 1447.
(13) Wei Z. G.; Sun L. D.; Liao C. S.; Yin J. L.; Jiang X. C.; Yan C. H.; Lü, S. Z. *J. Phys. Chem. B* **2002**, *106*, 10610.
(14) Davis S. A.; Breulmann M.; Rhodes K. H.; Zhang B.; Mann S. *Chem. Mater.* **2001**, *13*, 3218.
(15) Wegh R. T.; Donker H.; Oskam K. D.; Meijerink A. *Science* **1999**, *283*, 663.
(16) Feldmann C.; Jüstel T.; Ronda C. R.; Wiechert D. U. *J. Lumin.* **2001**, *92*, 245.
(17) Judd B. R. *Phys. Rev.* **1962**, *127*, 750.